Published in final edited form as:

J Am Coll Cardiol. 2020 January 07; 75(1): 1–13. doi:10.1016/j.jacc.2019.10.046.

Persistent Pro-arrhythmic Neural Remodeling Despite Recovery from Premature Ventricular Contraction-Induced Cardiomyopathy

Alex Y Tan, MD[1,2], **Khalid Elharrif, MD**[1,2], **Ricardo Cardona Guarache, MD, MPH**[1,2], **Pranav Mankad, MD**[1,2], **Owen Ayers**[2], **Martha Joslyn, MS**[2], **Anindita Das, PhD**[1], **Karoly Kaszala, MD, PhD**[1,2], **Shien-Fong Lin, PhD**[3], **Kenneth A. Ellenbogen, MD**[1,2], **Anthony J. Minisi, MD**[1,2], **Jose F. Huizar, MD**[1,2]

[1]Pauley Heart Center, Virginia Commonwealth University, Richmond, VA

[2]Electrophysiology Section, Division of Cardiology, Hunter Holmes McGuire VA Medical Center, Richmond, VA

[3]Krannert Institute of Cardiology, Indiana University School of Medicine, Indianapolis, IN.

Abstract

Background—The presence and significance of neural remodeling in premature ventricular contraction-induced cardiomyopathy (PVC-CM) remain unknown.

Objectives—To characterize cardiac sympatho-vagal balance and pro-arrhythmia in a canine model of PVC-CM.

Methods—In 12 canines, we implanted epicardial pacemakers and radiotelemetry unit to record cardiac rhythm and nerve activity (NA) from the left stellate ganglion (SNA), left cardiac vagus (VNA) and arterial blood pressure. Bigeminal PVCs (200ms coupling) were applied for 12-weeks to induce PVC-CM in 7 animals then disabled for 4-weeks to allow complete recovery of left ventricular ejection fraction (LVEF), vs 5 sham-controls.

Results—After 12 weeks of PVCs, LVEF (p=0.006) and dP/dT (p=0.007) decreased. Resting SNA (p=0.002) and VNA (p=0.04), exercise SNA (p=0.01), SNA response to evoked PVCs (p=0.005), heart rate (HR) at rest (p=0.003) and exercise (p<0.04) increased, while HR variability (HRV) decreased (p=0.009). There was increased spontaneous atrial (p=0.02) and ventricular arrhythmias (p=0.03) in PVC-CM. Increased SNA preceded both atrial (p=0.0003) and ventricular (p=0.009) arrhythmia onset. Clonidine suppressed SNA and abolished all arrhythmias. After disabling PVC for 4 weeks, LVEF (p=0.01), dP/dT (p=0.047) and resting VNA (p=0.03) recovered to baseline levels. However, SNA, resting HR, HRV and atrial (p=0.03) and ventricular (p=0.03) pro-arrhythmia persisted. There was sympathetic hyperinnervation in stellate ganglia (p=0.02) but not ventricles (p=0.2) of PVC-CM and recovered animals vs sham controls.

Address Correspondence to: Alex Y. Tan, MD, Electrophysiology Section, Division of Cardiology, Hunter Holmes McGuire VA Medical Center, 1201 Broad Rock Blvd, Richmond, VA 23220, Telephone: 804 675 5466, Fax: 804 675 5467, alex.tan@va.gov, Twitter: @RichmondVAMC.

Conclusion—Neural remodeling in PVC-CM is characterized by extracardiac sympathetic hyperinnervation and sympathetic neural hyperactivity that persists despite normalization of LVEF. The altered cardiac sympatho-vagal balance is an important trigger and substrate for atrial and ventricular pro-arrhythmia.

Condensed Abstract

The presence and significance of neural remodeling in premature ventricular contraction-induced cardiomyopathy (PVC-CM) remain unknown. In a canine model of PVC-CM, we demonstrated evidence of sympathetic neural hyperactivity, extracardiac sympathetic hyperinnervation and atrial and ventricular pro-arrhythmia that persisted despite complete recovery of left ventricular systolic function after PVCs were disabled. In contrast, vagal nerve activity increased with development of PVC-CM, but recovered to baseline levels upon resolution of PVC-CM. We conclude that neural remodeling and altered cardiac sympatho-vagal balance provided a trigger and substrate for atrial and ventricular pro-arrhythmia, and may be important in the pathogenesis of PVC-CM.

Keywords

Autonomic nervous system; non-sustained ventricular tachycardia; idiopathic ventricular arrhythmia; cardiomyopathy

Introduction

Frequent premature ventricular contractions (PVCs) can cause a non-ischemic cardiomyopathy (CM) (1) resulting in systolic heart failure. (2) PVC-induced CM (PVC-CM) is a unique form of CM characterized by LV systolic dysfunction that is reversible upon successful PVC suppression. (1, 2) (3) However, lethal ventricular arrhythmias and sudden cardiac death have been reported in patients with PVC-CM. (4) Autonomic imbalance, specifically sympathetic upregulation, has been postulated to contribute both to the pathogenesis of PVC-CM and its pro-arrhythmic consequences. The hypothesis is based upon studies demonstrating PVCs as a powerful acute stressor of the cardiac autonomic nervous system (CANS) (5,6). However, longer term CANS function of the CANS when exposed to chronic PVCs, and its relationship with arrhythmogenesis, remain unknown. We recently reported that application of chronic bigeminal PVCs in a canine model for 12 weeks (7,8) resulted in PVC-CM that was fully reversible 4-weeks after disabling PVCs. The goal of the present study was to perform chronic, ambulatory recordings of cardiac sympathetic and vagal nerve activity (9) in our canine model of PVC-CM to characterize cardiac sympatho-vagal balance and arrhythmogenesis during the development and subsequent resolution of PVC-CM. We hypothesize that neural remodeling occurs in PVC-CM, resulting in elevation in cardiac sympathetic tone which in turn is pro-arrhythmic.

Methods

The protocol was approved by the Institutional Animal Care and Use Committee and conformed to the National Institute of Health's Guide for the Care and Use of Laboratory Animals. We studied 12 Mongrel canines (20–30kg), consisting of 7 experimental animals and 5 sham controls. Figure 1A diagrams the experimental protocol. The experimental group

underwent chronic bigeminal PVC exposure for 12 weeks then disabled for 4 weeks to allow LV function to recover.(7) Sham controls underwent identical first surgery and chronic instrumentation as the experimental group, followed by serial assessments of NA at 2, 4 and 8 weeks during SR without PVCs, prior to final surgery.

First Surgery

We implanted a bipolar epicardial pacing electrode (Boston Scientific, Minneapolis, Minnesota) in the right ventricular (RV) apex and connected it to a pacemaker (St. Jude Medical, St. Paul, Minnesota) as described previously (7). We also implanted a radiotelemetry device (Data Sciences International, Minneapolis, MN) to record NA (Figure 1B) from the left stellate ganglion (SNA), cardiac branch of the left thoracic vagus nerve (VNA), ECG and central arterial blood pressure (9). Please refer to supplemental methods for details.

Autonomic Nerve Data Acquisition and Analyses

Following two weeks of postoperative recovery (Figure 1A), NA, BP and ECG were acquired for 72 hours in sinus rhythm (SR) (baseline). Bigeminal PVCs (coupling 200 ms, Figure 1C) was then enabled for 12 weeks in the experimental group using a novel premature pacing algorithm. (7) PVCs were disabled after the development of PVC-CM confirmed by transthoracic echocardiography.(7) Telemetry recordings were repeated for 72 hours in SR (PVC-CM). PVCs remain disabled for a further 4 weeks to allow full recovery of LV systolic function (7). Following this, 72-hour recordings were repeated in SR (recovery). The methods for quantifying NA have been reported previously(9) and detailed in supplemental methods.

Pharmacologic validation of neural recordings

We performed pharmacologic challenges with intravenous clonidine (10 μg/kg) and phenylephrine (0.1 mg) to further verify that our recordings represented efferent sympathetic and vagal nerve traffic respectively. Please refer to supplemental methods.

Transthoracic Echocardiography and Exercise Tolerance test (ETT)

Echocardiography (Vivid-7, GE-Echopac Version 7.3.0, GE Medical Systems, Boston, Massachusetts) was performed in SR as described previously and expanded in supplemental methods (7,8).

Spontaneous Arrhythmias

We manually analyzed 24-hour periods of SR during baseline, PVC-CM and recovery, to determine the incidence of spontaneous atrial and ventricular arrhythmias. Please refer to supplemental methods for details.

Acute PVC Challenge

We determined the autonomic response to acute PVC challenge during baseline, PVC-CM and recovery. Animals were exposed to 1 minute of quadrigeminal PVCs (200ms coupling).

NA and systolic BP were quantified in 30-sec segments, before and after PVC onset. Please refer to expanded methods.

Final Surgery

A left thoracotomy was created. Animals were euthanized. Tissues were harvested and preserved in 4% formaldehyde overnight and stored in 70% alcohol until histological processing.

Histology

Ventricular (right ventricle, left ventricular free wall and apex) and neural tissue (left and right SG, left cardiac vagus) from the 7 animals in the experimental cohort (recovered PVC-CM), 5 sham normal controls and 5 historical unrecovered PVC-CM controls, were paraffin embedded, cut into 5 μm sections, mounted on glass slides and examined under light microscopy. The unrecovered PVC-CM controls underwent a similar chronic PVC protocol as the experimental group but without a recovery phase. The sections were stained with hematoxylin and eosin and Mason's trichrome and immunostained with Tyrosine Hydroxylase (TH) and Choline Acetyltransferase (ChAT) antibodies to highlight adrenergic and cholinergic neurons respectively.(10) Quantitative analyses of immunostaining (TH, ChAT) and myocardial fibrosis (Mason's trichrome) was performed using Image J software (NIH Java version 1.8.0).

Statistical analyses

Data was expressed as mean ± SEM. Repeated measures ANOVA (with Bonferroni posthoc analyses) was used to compare the means between baseline, PVC-CM and recovery. For non-parametric comparisons, a χ^2 test was used. A p-value <0.05 was considered statistically significant.

Results

The study period was 152±3 days for the experimental group and 58±2 days for the sham control group. After 12-weeks of bigeminal PVC exposure, all experimental animals developed PVC-CM (Figure 1D). Table 1 summarizes all results. Figure 1D illustrates the serial changes in LVEF (p=0.006) and dP/dT (p=0.007) which decreased significantly in PVC-CM compared with baseline. After disabling PVCs for 4-weeks, LVEF (p=0.001 vs PVC-CM, P=0.38 vs baseline) and dP/dT (p=0.046 vs PVC-CM, p=0.31 vs baseline) recovered to baseline values. LVEDV (Table 1) remained increased (p=0.029 vs baseline).

Pharmacologic Validation of Neural Recordings

Please refer to supplemental material for details.

Autonomic Nerve Activity at Rest

Figure 2 demonstrates diurnal profiles of resting SNA (**A**) and VNA (**B**) in SR at 3 stages: baseline, PVC-CM and recovery. Figure 2C demonstrates mean 24-hr resting SNA and VNA in experimental vs sham control groups. Table 1 summarizes the NA averages as well as mean resting HR and HRV of experimental group. There was a significant increase in SNA

(p=0.002) and VNA (p=0.04) in PVC-CM compared with baseline, and correlated with increased mean resting HR (p=0.037) and reduced HRV (p=0.009). After LVEF recovery, resting SNA decreased compared to PVC-CM (p=0.009) but not to baseline levels (p=0.004 vs baseline). In contrast, resting VNA recovered fully to baseline levels (p=0.035 vs PVC-CM, p=0.15 vs baseline). However, mean resting HR (p=0.04) remained elevated and HRV (p=0.045) remained decreased compared with baseline. In contrast, resting SNA and VNA in the sham control group were unchanged through weeks 2, 4, and 8 after first surgery (p=0.79).

Autonomic Nerve Activity during Exercise treadmill test (ETT)

Figure 3A is a profile of SNA during 5-minutes pre-exercise, followed by a 9-minute ETT and subsequent 10-minute recovery in SR. Compared to baseline, mean exercise SNA during ETT was increased in PVC-CM (p<0.01, Figure 3B). Following recovery from PVC-CM, exercise SNA decreased compared with PVC-CM (p=0.014), but it remained elevated compared with baseline (p=0.048). Exercise VNA (Figure 3B) was also increased in PVC-CM (p=0.01) compared with baseline. Unlike SNA, exercise VNA was restored to baseline levels (p=0.21) in recovered PVC-CM. Mean (p=0.037) and maximum HR (p=0.042) during exercise (**3B**) were both higher in PVC-CM compared with baseline. After recovery, mean (p=0.039 vs PVC-CM, p=0.44 vs baseline) and maximum (p=0.049 vs PVC-CM, p=0.17 vs baseline) exercise HR recovered to baseline levels.

Spontaneous Arrhythmias

Table 1 compares arrhythmia frequency between baseline, PVC-CM and recovery. Figure 4 illustrates an example of spontaneous paroxysmal atrial tachyarrhythmia (PAT) (**A**), non-sustained (<30-sec) ventricular tachycardia (NSVT) (**B**) and PVC (**C**). Note that there was increased SNA and VNA prior to PAT onset and increased SNA alone prior to VT or PVC onset. Figure 5A compares arrhythmia frequency at different stages. There was a significant increase in the incidence of PAT (p = 0.02) in PVC-CM compared with baseline. There was no difference in mean PAT cycle length (309±6 vs 291±12 ms, p = 0.09), but total PAT duration was longer in PVC-CM compared with baseline (1486±187 vs 710±204 sec, p = 0.004). Increased atrial arrhythmia burden persisted in recovery (frequency: 77±25 vs 34±10 episodes/day vs baseline, p=0.03; duration: 1125±198 vs 710±204 sec vs baseline, p=0.03). No animals had spontaneous ventricular arrhythmia at baseline, whereas spontaneous PVCs (total 34 episodes) and non-sustained VT (total 19 episodes) were observed in 3/7 animals during CM (PVCs: 20 episodes, NSVT: 10 episodes, p=0.03 vs baseline) and in 3/7 animals in recovery (PVCs: 14 episodes, NSVT: 9 episodes, p=0.03 vs baseline). No animals developed sustained (>30-sec) VT or sudden cardiac death.

Figure 5B summarizes NA quantitation at arrhythmia onset. There was a surge in SNA (p=0.0003) and VNA (p=0.004) within 10s of PAT onset (vs 60 s prior to onset). SNA increase preceded VNA increase by 20s (−30s vs −10s). SNA peak in the 10s prior to PAT onset was higher than mean daily 10s SNA levels during CM (214±44 vs 160±9μV.s, p=0.02). VNA peak prior to PAT onset (79±15 μV.s) was higher than mean daily 10s VNA levels at baseline (38±10 μV.s, p=0.004) but not CM (141±43 μV.s, p=0.1). In contrast to atrial arrhythmias, only SNA was significantly increased prior to ventricular arrhythmia

onset (Figure 5C). This increase occurred within 3s of arrhythmia onset (p=0.046 vs 5s prior to onset) and peaked within 1s of arrhythmia onset (p=0.009 vs 5s prior to onset). The peak SNA levels prior to ventricular arrhythmia onset was significantly higher than the mean daily 1s SNA levels (24±3 vs 7±2 μV.s, p=0.03). To determine whether NA was a trigger for arrhythmias, we administered intravenous (IV) clonidine (10μg/kg), a central imidazoline receptor antagonist known to suppress central sympathetic output, and monitored the frequency of arrhythmias within the first 4 hours of administration. This time period is equivalent to 12 distribution half-lives ($T_{1/2}$ = 20min) of IV clonidine, incorporates the peak clonidine effect (1 hour) and well within its 12-hour elimination half-life. IV clonidine significantly diminished both SNA (p<0.0001) (Supplementary Figure 1A) and abolished both atrial (p=0.0003) and ventricular arrhythmias (p=0.01) at all stages, including PVC-CM and recovery.

Autonomic Response to Acute PVC Challenge

Figure 6 illustrates the autonomic response to a 1-minute acute PVC challenge performed during SR at baseline, PVC-CM and recovery. Acute SNA discharge (**6A**) occurred within seconds after PVC onset. **6B** is a graphical representation of integrated SNA and VNA and mean systolic BP during each 5-sec period, before and after PVC onset. **6C** compares 5-sec integrated SNA and VNA and mean systolic arterial BP before and after PVC onset. There was increased SNA discharge in the 30-sec period after PVC onset. The acute SNA response to PVCs was greater and more sustained in PVC-CM compared with baseline. The VNA response was not significantly different after PVC onset. PVCs induced a significant increase in systolic BP in PVC-CM and recovery, but not at baseline.

Histology

Figure 7 illustrates TH immunostaining in the R and LSG (Figure 7A–C) in sham normal controls, PVC-CM, and recovered PVC-CM groups. There was a significant increase in TH immunoreactivity in both LSG (p=0.02) and RSG (p=0.008) of PVC-CM and recovered PVC-CM animals compared with sham normal controls (**7D**). There was no difference in TH immunoreactivity in the SG between PVC-CM vs recovered PVC-CM (p=0.7). In the ventricles (data representing mean of RV and LV regions), there was no significant difference in TH immunoreactivity (sham controls: 14±1.8 vs PVC-CM: 17.7±2.7 vs recovered PVC-CM: 13.9±2$\mu m^2/cm^2$, p=0.2) or interstitial fibrosis (**7E**) (sham controls: 24.1±7.3 vs PVC-CM: 32.4±6.3 vs recovered PVC-CM: 35.7±8.5$\mu m^2/cm^2$, p=0.1) between the three groups (control, PVC-CM, recovered PVC-CM).There was no difference in ChAT immunoreactivity in the left cardiac vagus nerve (**7F**) (control: 45.5±4.2$\mu m^2/cm^2$, PVC-CM: 49.9±6.3$\mu m^2/cm^2$, recovered PVC-CM: 51.5±6.4$\mu m^2/cm^2$, p=0.8). ChAT was non-immunoreactive in the ventricular myocardium.

Discussion

We report significant and dynamic alterations of cardiac autonomic balance in the development and subsequent resolution of PVC-CM.

1. SNA and VNA were both elevated in PVC-CM compared with baseline. However, increased resting and exercise HR and reduced heart rate variability (HRV) reflect net sympathetic dominance in PVC-CM.
2. Evoked RV apical PVCs (quadrigeminy, short coupled) triggered an acute increase in SNA but not VNA. In PVC-CM, the SNA response to PVCs was greater in magnitude and duration compared with baseline.
3. There was an increased incidence of spontaneous atrial and ventricular arrhythmias in PVC-CM compared with baseline. Increased SNA and VNA immediately preceded the onset of atrial arrhythmias whereas increased SNA immediately preceded onset of ventricular arrhythmias. Clonidine suppressed SNA and all arrhythmias in the setting of PVC-CM.
4. Upon complete LVEF recovery 4-weeks after disabling PVCs, VNA recovered to baseline levels but SNA remained elevated at rest, exercise and in response to evoked PVCs, causing persistent sympathetic imbalance, elevated resting HR, suppressed HRV and lack of recovery of pro-arrhythmia.
5. Histology demonstrated sympathetic hyperinnervation limited to stellate ganglia sparing ventricular myocardium in PVC-CM. Stellate ganglia hyperinnervation persisted in recovered PVC-CM.

Taken together, these data provide evidence of neural remodeling of the stellate ganglia in PVC-CM. This remodeling persists beyond the complete recovery of LV systolic function and maintains a state of heightened cardiac sympathetic tone and pro-arrhythmia. These findings may have implications for patients with PVC-CM despite successful PVC suppression strategy.

Neural Remodeling in PVC-CM

After the development of PVC-CM, there were significant changes to SNA, VNA and HR (Figures 2 and 3) that reflect net sympathetic dominance. To our best knowledge, this is the first demonstration of chronic sympathetic upregulation in PVC-CM. The fact that SNA upregulation persisted despite LVEF and dP/dT recovery indicates that neural remodeling has occurred in PVC-CM. On the other hand, VNA was also upregulated in PVC-CM but recovered to baseline levels after CM resolution. VNA recovery tilted autonomic balance in favor of sympathetic dominance in recovered PVC-CM. In contrast to the experimental group, the lack of change of NA in sham control group over 8 weeks indicate that the changes of NA in the experimental group were due to development of PVC-CM not post-surgical changes. It is important to note that NA quantitation during rest and exercise were obtained in SR rather than during PVCs, in order to evaluate NA-HR coupling not otherwise possible with frequent PVCs. Therefore, chronic sympathetic upregulation in PVC-CM is not due to the acute effects of PVCs. Rather, they reflect a remodeled CANS reset to chronically higher SNA output by chronic PVC exposure but are independent of PVCs themselves. On the other hand, the acute effects of PVCs on NA were evaluated separately (Figure 6) and discussed further below. One advantage of our PVC-CM model is the ability to determine whether NA recovers in parallel with LVEF. We note that the increase in SNA tracked reductions in LVEF and dP/dT, and conversely, partial SNA recovery was associated

with resolution of LV dysfunction, suggesting that SNA changes are in part a dynamic adaption to the mechanical cardiac dysfunction caused by PVCs. However, the incompleteness of SNA recovery also suggests that the mechanism of sympathetic upregulation in PVC-CM is unique to PVC-CM and not solely related to LV dysfunction per se. Conversely, SNA changes may also contribute to the pathogenesis of PVC-CM, a potentially important therapeutic prospect that merits further exploration.

Mechanisms of Acute Sympathetic Pertubation by PVCs

PVCs are hypothesized to provoke the CANS via a complex neural reflex pathway involving arterial and cardiac baroreceptors and intrinsic cardiac autonomic nerves that feedback on efferent nerves in the extrinsic CANS to regulate the cardiac response. (5) (11) Muscle sympathetic nerve recordings in humans demonstrated that burst sympathetic nerve discharge initiates at the diastolic pressure nadir following a PVC beat due to baroreceptor deactivation, and terminates with the systolic peak of the post-PVC beat(12) due to baroreceptor activation that inhibits efferent sympathetic outflow. In an in-vivo porcine model, Hamon et al(5) demonstrated that acute PVCs, especially those with variable coupling, cause potent firing of intrinsic cardiac autonomic nerves. Smith et al. (6) found that frequent PVCs trigger increased muscle sympathetic nerve activity and coronary sinus norepinephrine levels. However, the acute and chronic effects of PVCs on sympatho-vagal nerve activity in normal and PVC-CM hearts, remain unknown. In normal hearts (baseline), short term PVC application triggers an acute increase in SNA but not VNA (Figure 6A). This was accompanied by a gradual increase in BP (**6B**) due to post-extrasystolic potentiation, (13) which in turn moderated further SNA increases via baroreflex activation. (14) However, the SNA response to PVCs was greater in amplitude and duration in PVC-CM compared with normal hearts. This is despite a greater increase in BP (Figure 6B and C) which would have otherwise tempered SNA increase via baroreflex activation. (14) Increased SNA response to PVCs persisted in recovered PVC-CM hearts when compared to baseline (normal hearts). These data suggest that baroreflex blunting has occurred in PVC-CM. Because our studies were performed in a non-anesthetized state, the results reflect real-life autonomic physiology conducive to baroreflex assessment. We conclude that PVCs perturb the CANS by a complex interplay of mechanisms that trigger SNA by baroreflex deactivation then suppress SNA by baroreflex activation. This dynamic balance of opposing forces becomes altered in PVC-CM and remains altered despite LV function recovery. We propose that neural remodeling in the CANS (i.e. sympathetic hyperinnervation in the stellate ganglia) increases the magnitude of SNA response to PVCs whereas baroreflex blunting results in a more prolonged SNA response to PVCs. Baroreflex blunting carries an adverse prognosis in patients with heart disease, (15) underscoring the potential significance of neural remodeling and baroreflex alteration in current or recently recovered PVC-CM.

Pro-arrhythmia and Neural Remodeling

The presence and arrhythmogenic significance of chronic sympathetic upregulation in PVC-CM remain unknown. In the present study, we report increased burden of both atrial and ventricular arrhythmias in PVC-CM. There was a significant temporal correlation between ventricular arrhythmia onset and SNA increase, and between atrial arrhythmias and acute SNA and VNA increase, suggesting that the arrhythmias are neurally triggered. Clonidine,

an inhibitor of central sympathetic output, (16) significantly diminished SNA and abolished these arrhythmias after PVC-CM developed. These data indicate that SNA is a critical trigger for both atrial and ventricular arrhythmias in PVC-CM. In addition to an arrhythmic trigger, sympathetic neural remodeling creates a pro-arrhythmic substrate in PVC-CM. We hypothesize that this substrate derives from critical interactions between elevated sympathetic tone with cellular electrophysiological remodeling in PVC-CM. The latter includes heterogeneous reductions of IK_1, ICa_L and I_{to}, leading to increased dispersion of ventricular action potential duration and refractoriness as we previously reported.(17) In electrophysiologically remodeled hearts, PVCs in the presence of sympathetic stimulation induces greater beat-to-beat electrical conduction and repolarization abnormalities than in normal hearts. (18) Conversely, we demonstrated that neural remodeling promoted greater PVC burden and greater sympathetic responses to evoked PVCs. Therefore, the combination of neural and electrical remodeling in PVC-CM may lead to a vicious cycle and perfect storm for malignant ventricular arrhythmias.

Role of Neural Remodeling in Pathogenesis of PVC-CM

Although chronic sympathetic upregulation is present in PVC-CM, it remains unclear whether it is a cause or effect of PVC-CM. We previously reported in our canine PVC-CM model, decreases in L-type calcium channel current and protein subunit, decreases in calcium-induced calcium release and dyad scaffolding protein, junctophilin. (17) On the other hand, sympathetic stimulation increases L-type calcium current by beta-receptor stimulated cyclic AMP-dependent phosphorylation of L-type calcium channel thus increasing cardiac inotropy. (19) Therefore, sympathetic upregulation may be a compensatory mechanism for abnormal calcium handling and LV systolic dysfunction in PVC-CM. However, sympathetic upregulation itself has been shown to depress myocardial function via the direct toxic effects of norepinephrine on cardiac myocytes with resulting necrosis and apoptosis and impaired beta-adrenoreceptor function. (20) Another potential pathophysiologic link between sympathetic upregulation and PVC-CM is via pro-arrhythmia. Neural remodeling promotes increased PVCs (and other arrhythmias), which in turn trigger increased SNA, leading to a vicious cycle of pro-arrhythmia and arrhythmia-induced CM (PVC-CM vs tachycardia-induced CM), regardless of the initiating stimulus. (3) Further studies are needed to clarify the role of sympathetic neural remodeling in the pathogenesis of PVC-CM.

Stellate ganglia neural remodeling

Our histology studies indicate that neural remodeling is limited to the stellate ganglia sparing the cardiac vagal nerve and sympathetic nerves within the ventricular myocardium. This is in contrast to tachypacing models of cardiomyopathy (21) or to human systolic heart failure (22) which are characterized by significant sympathetic hyperinnervation within the heart. The differences in neural, electrophysiological and structural remodeling between PVC-CM(7, 17) and conventional models(21, 22) of systolic cardiomyopathy, suggest that the mechanisms of remodeling in PVC-CM are unique to PVC-CM. The sparing of ventricular myocardium in PVC-CM could also be due to the less severe extent of LV dysfunction compared to tachypacing models, evidenced by the absence of clinical heart failure and normal pro-BNP levels in our model, (8) or to the relatively short duration of

exposure to PVCs. On the other hand, the absence of remodeling of the vagus may contribute to sympathetic excess in PVC-CM and after its recovery. Remodeled stellate ganglia could be a pro-arrhythmic substrate and thus a potential therapeutic target for PVC-CM, similar to left cardiac sympathetic denervation for ventricular arrhythmia storm. (23).

Limitations

The intrinsic CANS has been shown to be an important modulator of cardiac response to PVCs. (5) We, however, did not record NA from the intrinsic CANS in this study. We also did not measure serum norepinephrine levels. We selected 4-weeks as an appropriate time course for recovery of LVEF, based on previous findings. (7) However, a longer study may be necessary to determine if further recovery of SNA occurs. Our animal model was limited by the use of fixed coupled PVCs from the RV apex. Although our data suggests an important pathophysiologic role of neural remodeling in PVC-CM, whether elevated sympathetic tone per se is causative of PVC-CM remains unresolved.

Conclusions

Neural remodeling in PVC-CM is characterized by extracardiac sympathetic hyperinnervation resulting in imbalanced sympathetic neural hyperactivity, increased atrial and ventricular pro-arrhythmia and exaggerated sympathetic firing in response to PVCs. This sympatho-vagal imbalance and pro-arrhythmia persist despite resolution of PVC-CM.

Supplementary Material

Refer to Web version on PubMed Central for supplementary material.

Acknowledgments

The authors acknowledge Marcus Thames, MD, for his helpful review of the manuscript.

Funding: A.Y.T receives research grants from American Heart Association (AHA SDG 16SDG31280012); J.F.H receives research grants from National Institutes of Health (1R56HL133182-01).

Disclosures: Kaszala K – Research support from Boston Scientific Corp (BS) and St. Jude Medical (SJM); Ellenbogen KA – Research support from BS, Biosense Webster (BW), Medtronic (MDT), SJM, Consultant for BS, SJM, Atricure, MDT, Honoraria from MDT, BS, BTK, BW and Atricure; Huizar JF – Research support from SJM. The remaining authors have nothing to disclose.

Abbreviations

NA	nerve activity
SNA	sympathetic NA
VNA	vagal nerve activity
CANS	cardiac autonomic nervous system
PVC-CM	premature ventricular complex
PVC	induced cardiomyopathy

LVEF	left ventricular ejection fraction
SR	sinus rhythm

References

1. Yarlagadda RK, Iwai S, Stein KM, et al. Reversal of cardiomyopathy in patients with repetitive monomorphic ventricular ectopy originating from the right ventricular outflow tract. Circulation 2005;112:1092–1097. [PubMed: 16103234]
2. Penela D, Van Huls Van Taxis C, Van Huls Vans Taxis C, et al. Neurohormonal, structural, and functional recovery pattern after premature ventricular complex ablation is independent of structural heart disease status in patients with depressed left ventricular ejection fraction: a prospective multicenter study. J. Am. Coll. Cardiol 2013;62:1195–1202. [PubMed: 23850913]
3. Huizar JF, Ellenbogen KA, Tan AY, Kaszala K. Arrhythmia-Induced Cardiomyopathy: JACC State-of-the-Art Review. J Am Coll Cardiol 2019;73:2328–2344. [PubMed: 31072578]
4. Noda T, Shimizu W, Taguchi A, et al. Malignant entity of idiopathic ventricular fibrillation and polymorphic ventricular tachycardia initiated by premature extrasystoles originating from the right ventricular outflow tract. J. Am. Coll. Cardiol 2005;46:1288–1294. [PubMed: 16198845]
5. Hamon D, Rajendran PS, Chui RW, et al. Premature Ventricular Contraction Coupling Interval Variability Destabilizes Cardiac Neuronal and Electrophysiological Control: Insights From Simultaneous Cardioneural Mapping. Circ Arrhythm Electrophysiol 2017;10:e004937. [PubMed: 28408652]
6. Smith ML, Hamdan MH, Wasmund SL, et al. High-frequency ventricular ectopy can increase sympathetic neural activity in humans. Heart Rhythm 2010;7:497–503. [PubMed: 20184979]
7. Huizar JF, Kaszala K, Potfay J, et al. Left ventricular systolic dysfunction induced by ventricular ectopy: a novel model for premature ventricular contraction-induced cardiomyopathy. Circ Arrhythm Electrophysiol 2011;4:543–549. [PubMed: 21576277]
8. Tan AY, Hu YL, Potfay J, et al. Impact of ventricular ectopic burden in a premature ventricular contraction-induced cardiomyopathy animal model. Heart Rhythm 2015;0.
9. Tan AY, Zhou S, Ogawa M, et al. Neural mechanisms of paroxysmal atrial fibrillation and paroxysmal atrial tachycardia in ambulatory canines. Circulation 2008;118:916–925. [PubMed: 18697820]
10. Tan AY, Li H, Wachsmann-Hogiu S, Chen LS, Chen P-S, Fishbein MC. Autonomic innervation and segmental muscular disconnections at the human pulmonary vein-atrial junction: implications for catheter ablation of atrial-pulmonary vein junction. J Am Coll Cardiol. 2006;48:132–143. [PubMed: 16814659]
11. Lombardi F, Ruscone TG, Malliani A. Premature ventricular contractions and reflex sympathetic activation in cats. Cardiovasc. Res 1989;23:205–212. [PubMed: 2590904]
12. Smith ML, Ellenbogen KA, Eckberg DL. Baseline arterial pressure affects sympathoexcitatory responses to ventricular premature beats. Am. J. Physiol 1995;269:H153–9. [PubMed: 7543254]
13. Cooper MW. Postextrasystolic potentiation. Do we really know what it means and how to use it? Circulation 1993;88:2962–2971. [PubMed: 7504591]
14. Minisi AJ, Dibner-Dunlap M, Thames MD. Vagal cardiopulmonary baroreflex activation during phenylephrine infusion. Am. J. Physiol 1989;257:R1147–53. [PubMed: 2589540]
15. La Rovere MT, Bigger JT, Marcus FI, Mortara A, Schwartz PJ. Baroreflex sensitivity and heart-rate variability in prediction of total cardiac mortality after myocardial infarction. ATRAMI (Autonomic Tone and Reflexes After Myocardial Infarction) Investigators. Lancet 1998;351:478–484. [PubMed: 9482439]
16. Isaac L Clonidine in the central nervous system: site and mechanism of hypotensive action. J. Cardiovasc. Pharmacol 1980;(2 Suppl)1:S5–19.
17. Wang Y, Eltit JM, Kaszala K, et al. Cellular mechanism of premature ventricular contraction-induced cardiomyopathy. Heart Rhythm 2014;11:2064–2072. [PubMed: 25046857]

18. Vaseghi M, Lux RL, Mahajan A, Shivkumar K. Sympathetic stimulation increases dispersion of repolarization in humans with myocardial infarction. Am. J. Physiol. Heart Circ. Physiol 2012;302:H1838–46. [PubMed: 22345568]

19. Hartzell HC, Méry PF, Fischmeister R, Szabo G. Sympathetic regulation of cardiac calcium current is due exclusively to cAMP-dependent phosphorylation. Nature 1991;351:573–576. [PubMed: 1710784]

20. Floras JS. Sympathetic nervous system activation in human heart failure: clinical implications of an updated model. J Am Coll Cardiol 2009;54:375–385. [PubMed: 19628111]

21. Ogawa M, Zhou S, Tan AY, et al. Left stellate ganglion and vagal nerve activity and cardiac arrhythmias in ambulatory dogs with pacing-induced congestive heart failure. J Am Coll Cardiol. 2007;50:335–343. [PubMed: 17659201]

22. Cao JM, Fishbein MC, Han JB, et al. Relationship between regional cardiac hyperinnervation and ventricular arrhythmia. Circulation 2000;101:1960–1969. [PubMed: 10779463]

23. Ajijola OA, Wisco JJ, Lambert HW, et al. Extracardiac neural remodeling in humans with cardiomyopathy. Circ Arrhythm Electrophysiol 2012;5:1010–1116. [PubMed: 22923270]

24. Tan AY, Ellenbogen K. Ventricular Arrhythmias in Apparently Normal Hearts: Who Needs an Implantable Cardiac Defibrillator? Card Electrophysiol Clin 2016;8:613–621. [PubMed: 27521094]

25. Penela D, Fernández-Armenta J, Aguinaga L, et al. Clinical recognition of pure premature ventricular complex-induced cardiomyopathy at presentation. Heart Rhythm 2017;14:1864–1870. [PubMed: 28756100]

CLINICAL PERSPECTIVES

Competency in Patient Care and Procedural Skills

In patients with cardiomyopathy related to chronic premature ventricular contractions (PVC-CM), neural remodeling may result in a persisting pro-arrhythmic substrate despite PVC suppression.

Translational Outlook

Additional research is needed to develop novel therapeutic approaches aimed at preventing neural remodeling or modulating autonomic tone to reduce the risk of ventricular arrhythmias in patients with PVC-CM.

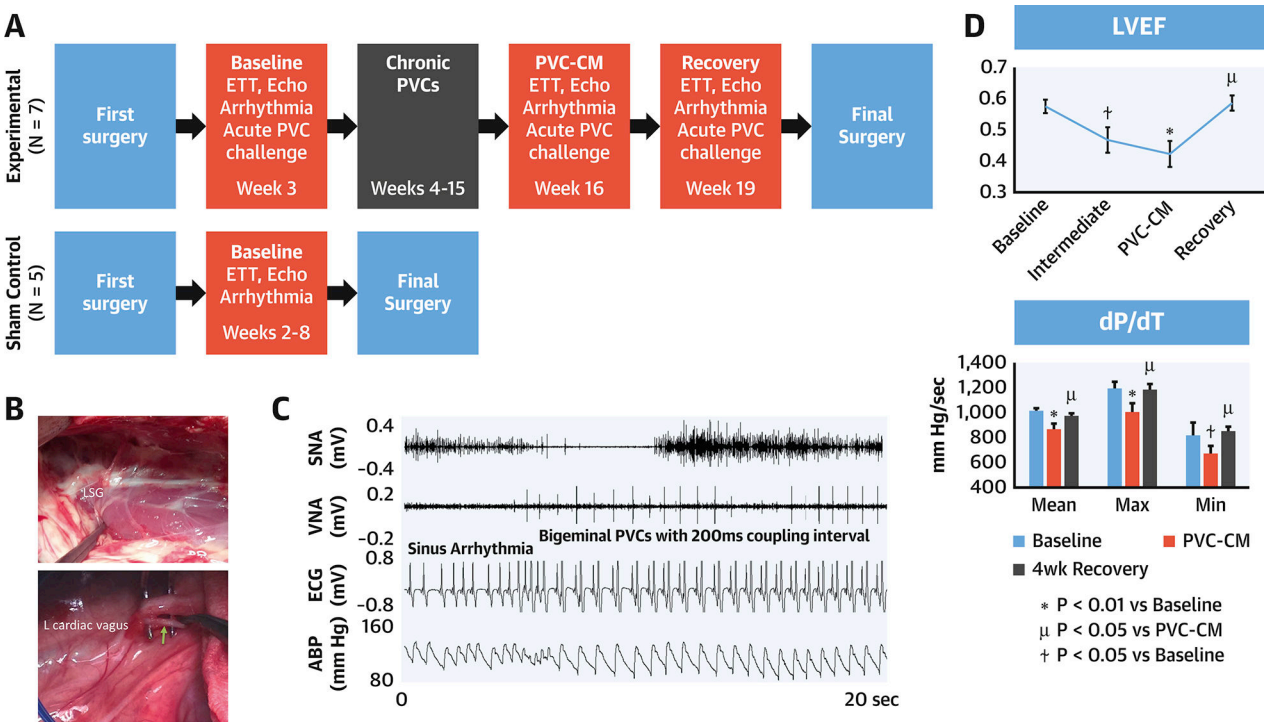

Figure 1. Experimental Protocol.

(**A**) Sequence of events. **(B)** Left thoracotomy showing left stellate ganglion and cardiac branch of left thoracic vagal nerve (arrow). **(C)** Initiation of bigeminal PVC associated with SNA increase. (**D**): Left ventricular ejection fraction (LVEF) and dP/dT during development of and recovery from PVC-induced cardiomyopathy (PVC-CM). Intermediate stage was obtained after 4-weeks of bigeminal PVC exposure. Abbreviations: SNA, sympathetic nerve activity; VNA, vagal NA; ABP, arterial blood pressure.

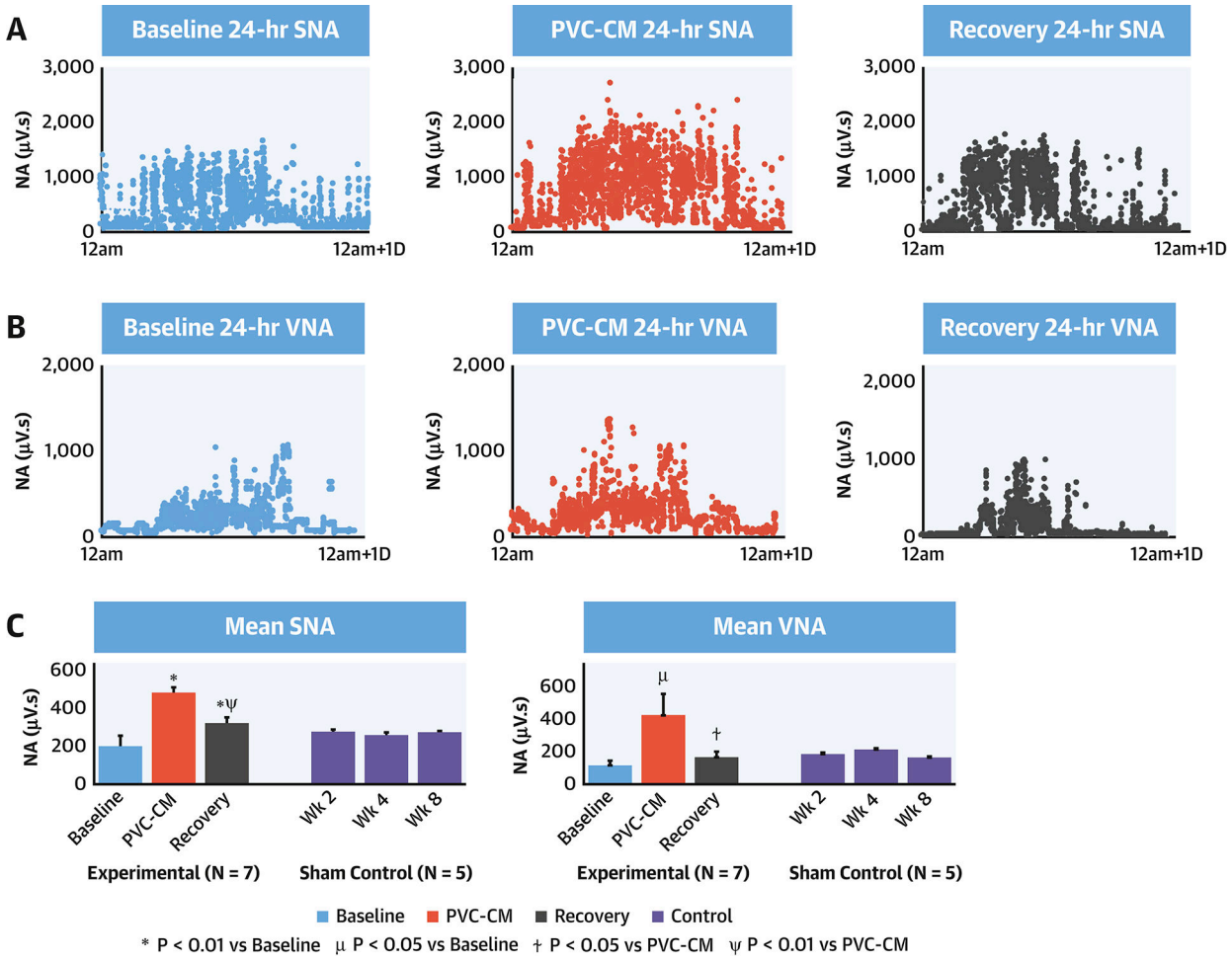

Figure 2. Changes in resting SNA and VNA with development of and recovery from PVC-CM.

Diurnal profiles of resting SNA **(A)** and VNA **(B)** during 24-hour of SR at baseline, PVC-CM and after recovery from PVC-CM. Every point represents 30-second integrated NA. **(C)** Mean 24-hour resting SNA and VNA in experimental vs sham control groups. ✻: P<0.01 vs Baseline, μ: P<0.05 vs Baseline, ψ: P<0.01 vs PVC-CM, †: P<0.05 vs PVC-CM.

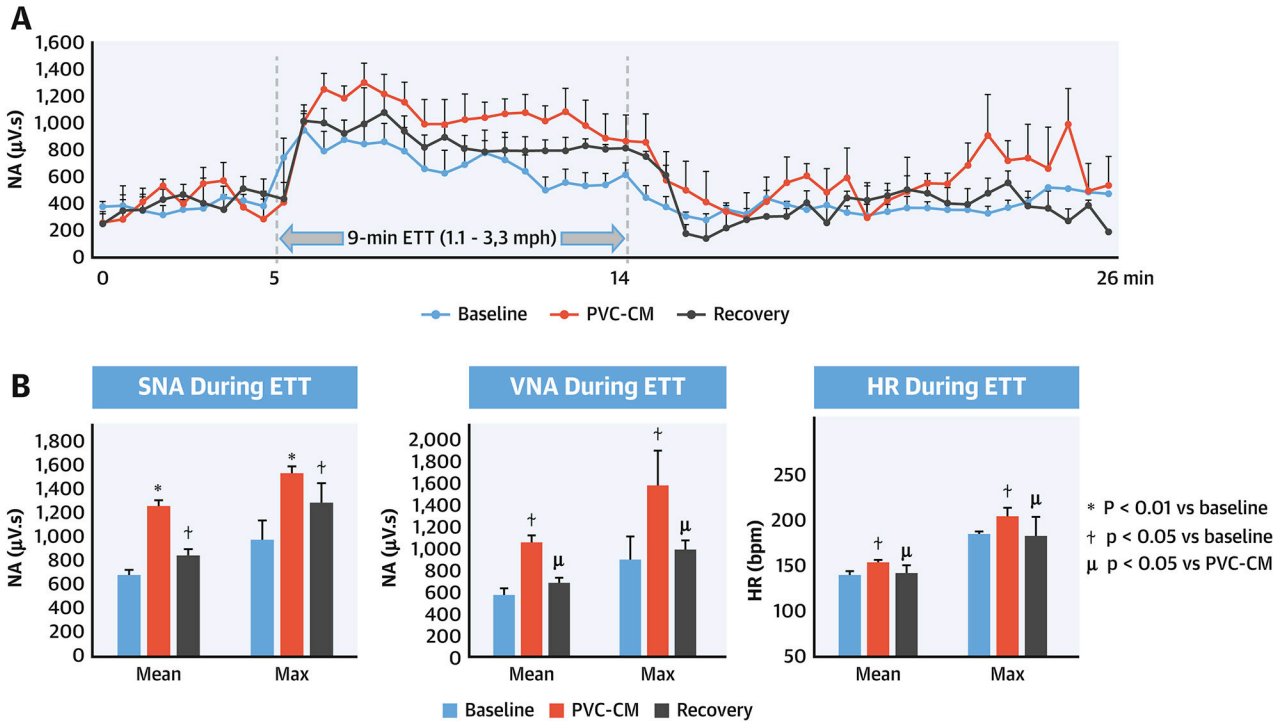

Figure 3. SNA response during exercise.

(**A**) SNA profile during ETT (up to 3.3mph). (**B**) Mean and maximal SNA, VNA and RR intervals during ETT.

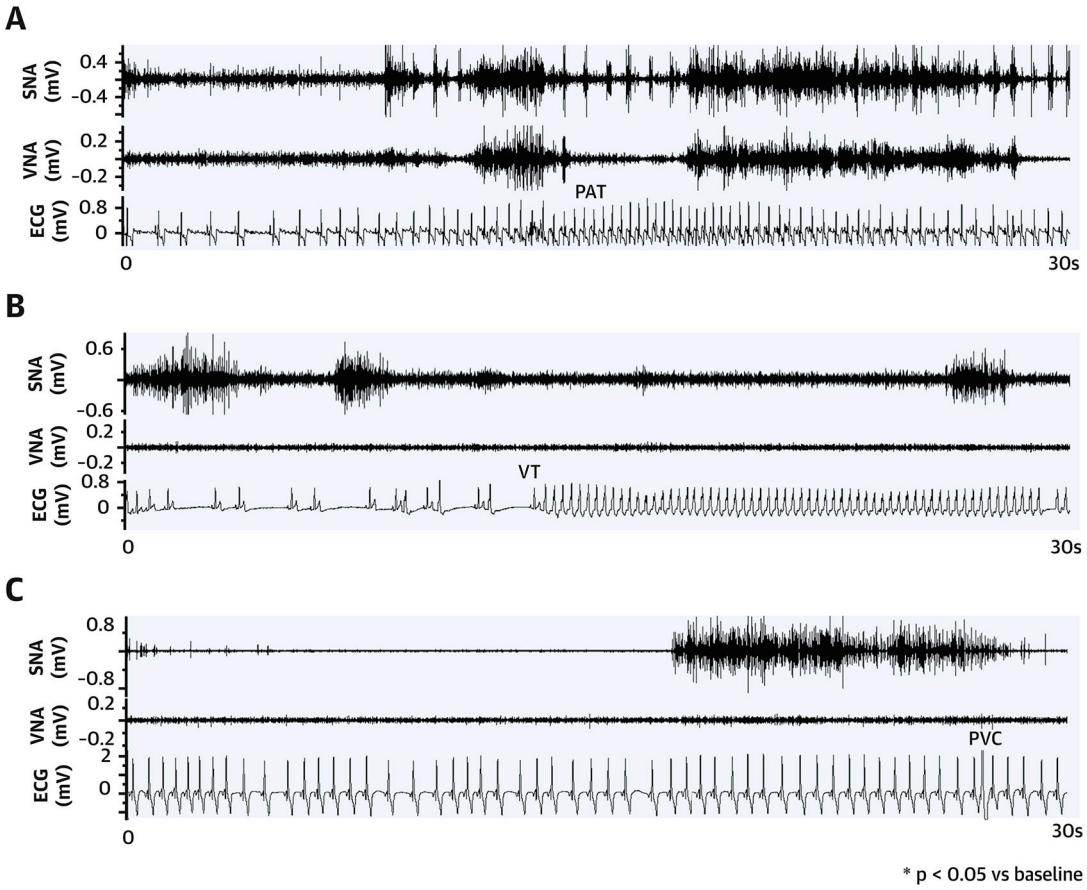

Figure 4. Neural triggers of atrial and ventricular arrhythmias in PVC-CM.

(A) Paroxysmal atrial tachyarrhythmia (PAT). **(B)** Non-sustained ventricular tachycardia (NSVT). **(C)** Premature ventricular contractions (PVCs).

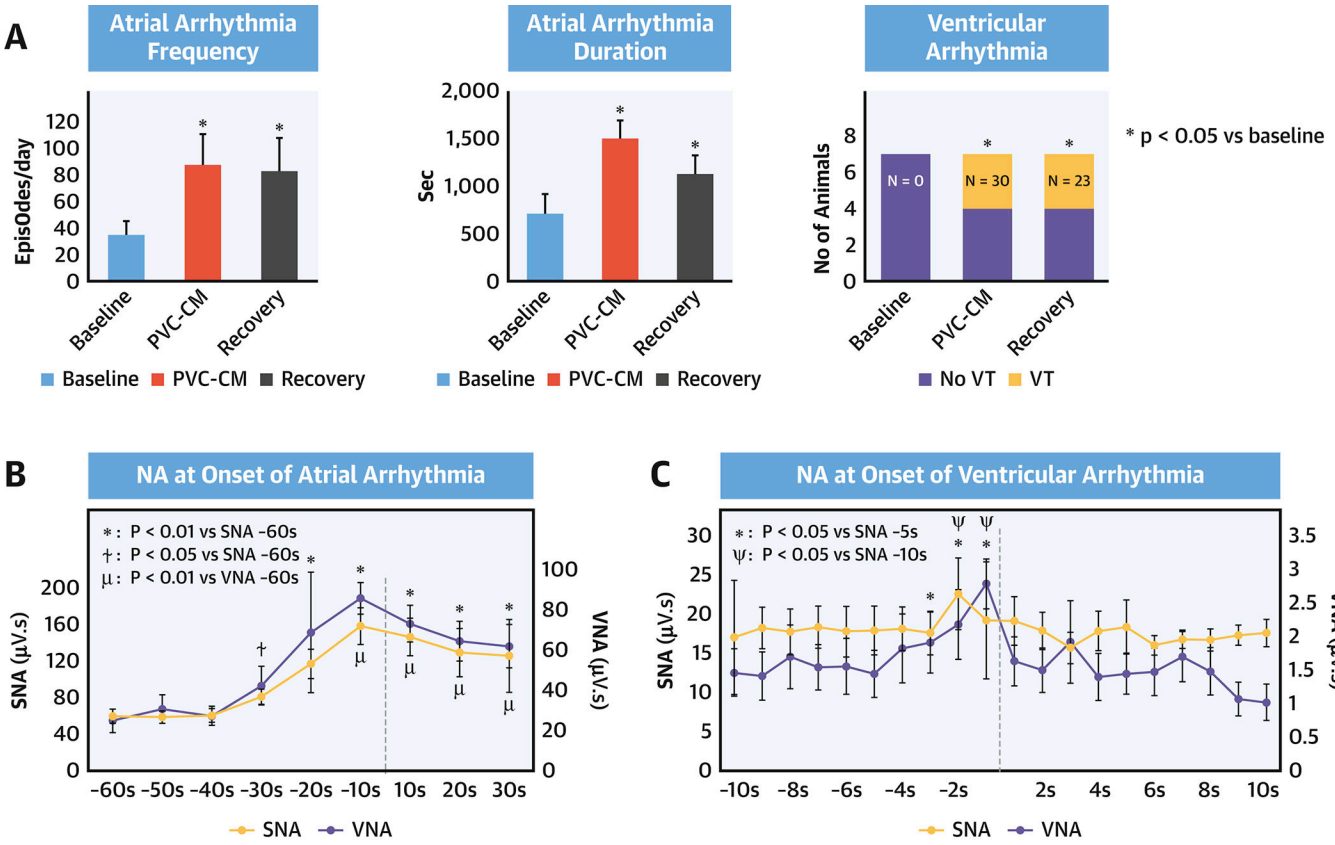

Figure 5. Pro-arrhythmia in PVC-CM and Recovery.

(A) Increased atrial and ventricular arrhythmia burden with PVC-CM and. Temporal relationship between autonomic nerve activity (NA) and onset of atrial **(B)** and ventricular **(C)** arrhythmia.

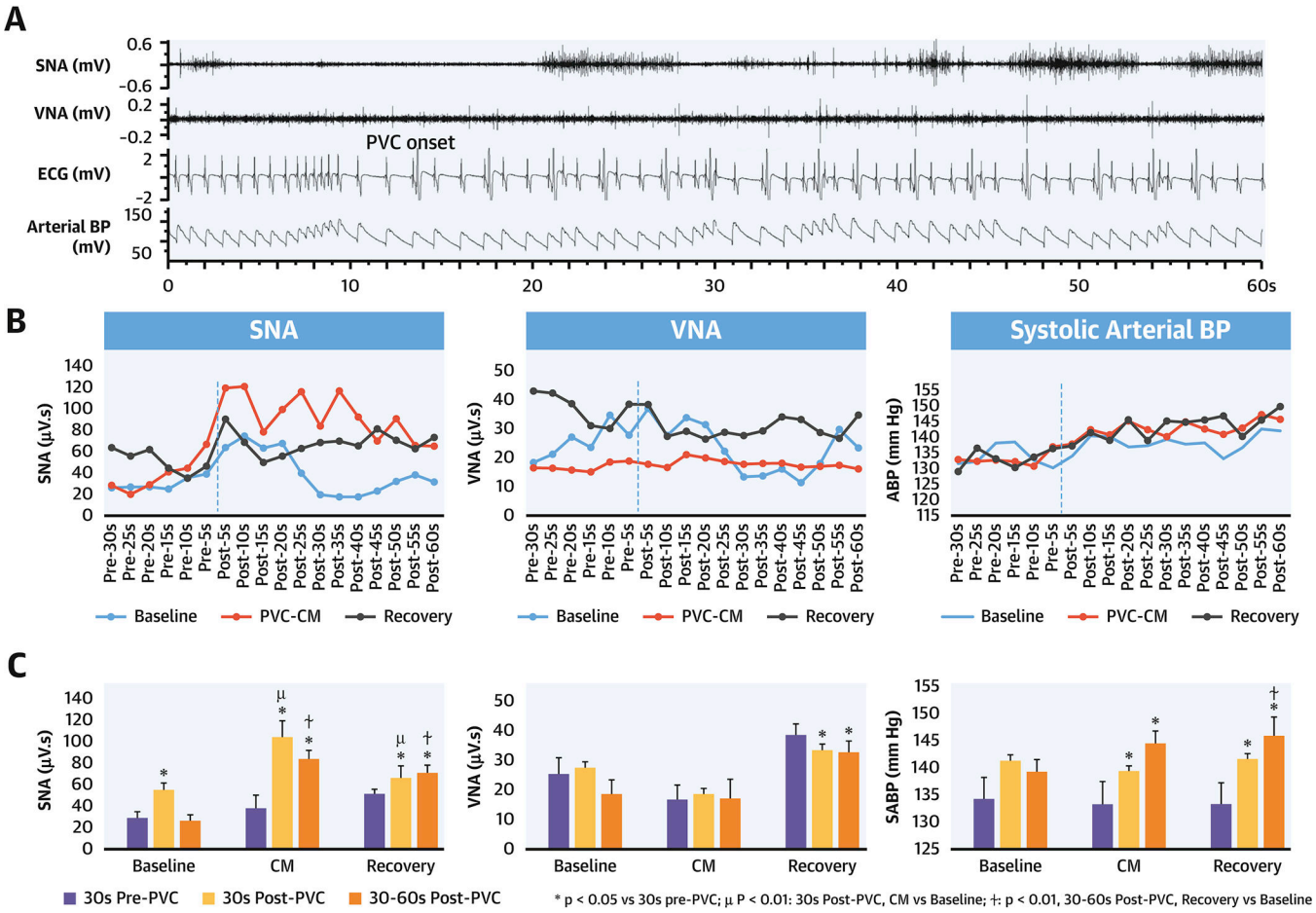

Figure 6. Effect of acute (1-minute) quadrigeminal PVC challenge (200 ms coupling) on NA and BP at baseline, PVC-CM and recovery.

(**A**) Acute SNA increase within seconds after PVC onset, followed by a slower rise in systolic BP. (**B**) Mean systolic BP and integrated NA over 5-sec period, before and after PVC onset. (**C**) Comparison of NA and mean systolic BP in 30-sec segments before vs after PVC onset.

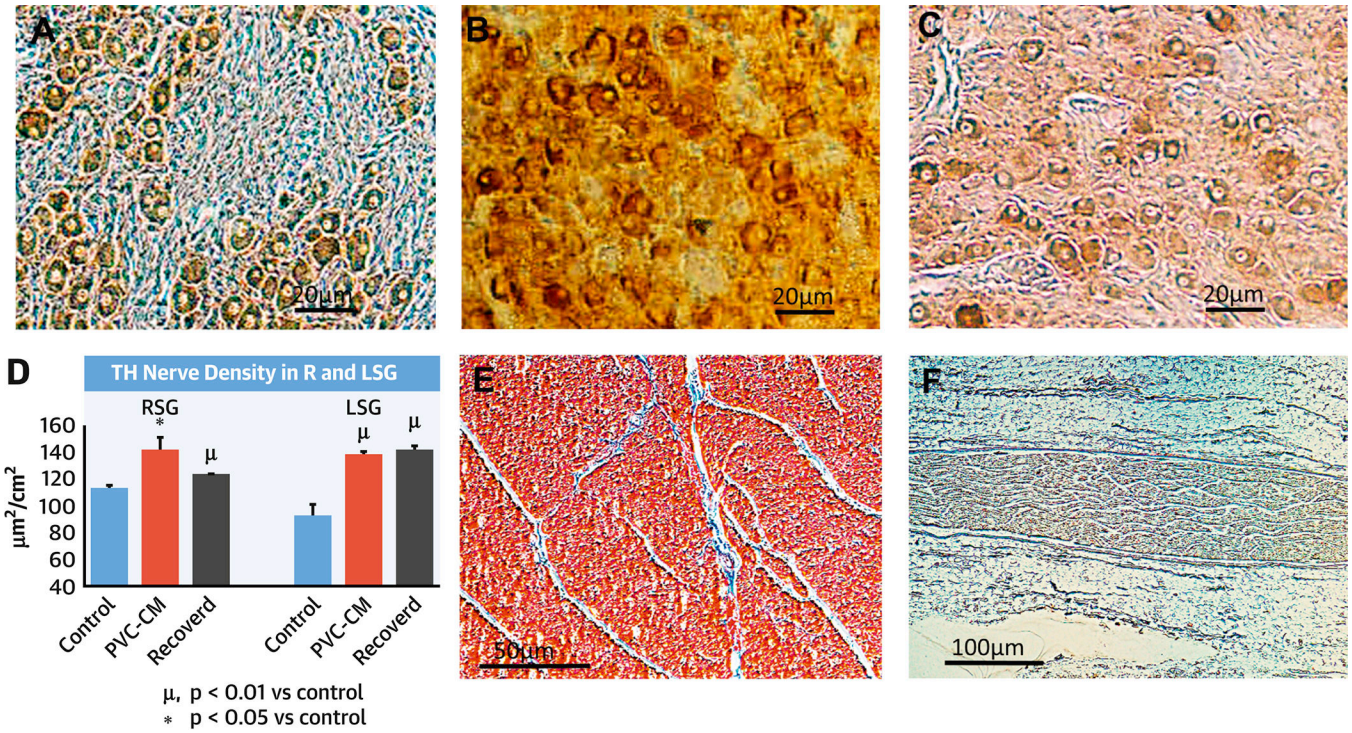

Figure 7. Sympathetic Neural Remodeling in PVC-CM.

Immunostaining with Tyrosine Hydroxylase (TH) antibodies of left and right stellate ganglia (LSG, RSG) in sham control (N=5), PVC-CM (N=5) and PVC-CM recovered (N=7) groups. (**A**) LSG Sham control. (**B**) LSG PVC-CM. (**C**) LSG Recovered PVC-CM. (**D**) Comparison of TH nerve density in R vs LSG. (**E**) Lack of interstitial fibrosis in PVC-CM. (**F**) Choline Acetyltransferase (ChAT) staining of L cardiac vagus nerve.

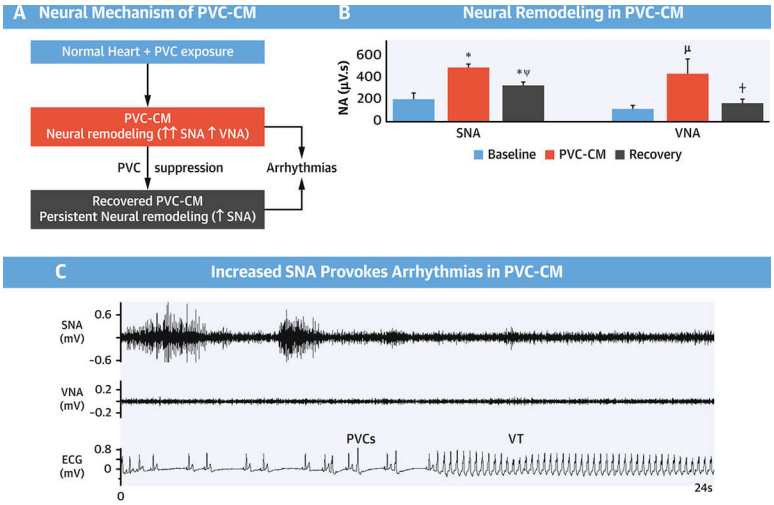

Central Illustration. Neural Remodeling in Premature Ventricular Contraction-Induced Cardiomyopathy.

(A) Proposed Neural Mechanism of Premature Ventricular Contraction-induced Cardiomyopathy (PVC-CM) and consequent pro-arrhythmia. Chronic frequent PVCs cause PVC-CM and neural remodeling. **(B)** Neural Remodeling in PVC-CM is characterized by increased SNA and VNA. Neural remodeling (increased SNA) persists despite recovery from PVC-CM. **(C)** In neurally remodeled hearts in PVC-CM and recovered PVC-CM, increased SNA triggers ventricular arrhythmias. ✻ $P<0.01$ vs Baseline; μ $P<0.05$ vs Baseline; ┼ $P<0.05$ vs PVC-CM; Ψ $P<0.01$ vs PVC-CM. Abbreviations: SNA, sympathetic nerve activity; VNA, vagal nerve activity; PVC-CM, premature ventricular contraction-induced cardiomyopathy; VT, ventricular tachycardia.

Table 1.

Results Summary.

Abbreviations: LVEF: left ventricular (LV) ejection fraction; LVEDV: LV end diastolic volume; dP/dT: rate of change of pressure with time; HR: heart rate; SNA and VNA: sympathetic and vagal nerve activity.

	Baseline	**PVC-CM** ***vs baseline***	**Recovery** ***vs baseline*** ***vs PVC-CM***
LVEF (%)	58±2	42±4 *P=0.006*	59±2 *P=0.38* *P=0.001*
LVEDV (ml)	47±2.8	61.4±4.6 *0.016*	56.7±2.3 *0.029* *0.17*
dP/dT (mmHg/s)	1015±24	870±40 *0.007*	977±21 *0.31* *0.046*
Mean Resting HR (bpm)	69±2	92±6 *0.004*	80±5 *0.04* *0.22*
Mean Exercise HR (bpm)	142±4	156±2 *0.037*	143±9 *0.44* *0.039*
Heart Rate Variability 24hr SDRR (s)	0.5±0.04	0.38±0.02 *0.009*	0.41±0.06 *0.045* *0.18*
Mean Resting SNA (μV.s)	199±5	480±28 *0.002*	320±31 *0.004* *0.009*
Mean Exercise SNA (μV.s)	698±38	1266±155 *0.014*	859±98 *0.048* *0.07*
Mean Resting VNA (μV.s)	115±30	423±129 *0.04*	165±33 *0.15* *0.03*
Mean Exercise VNA (μV.s)	566±44	1024±58 *0.025*	668±36 *0.21* *0.05*
Atrial tachyarrhythmia (episodes/day)	34±10	87±22 *0.02*	77±25 *0.03* *0.14*
Animals with Ventricular arrhythmia	0	3/7 (20 episodes) *0.03*	3/7 (19 episodes) *0.03* *1*